Rotordynamics of a Passive Magnet Bearing System

H. Ming Chen, Thomas Walter, Scott Wheeler, Nga Lee
Foster-Miller Technologies
431 New Karner Road, Albany, NY 12205-3868, USA
518-456-9919/518-456-8020
www.foster-miller.com

Keywords

active magnetic thrust bearing, active radial damper, passive radial bearing

Abstract

A passive magnetic bearing system is being developed for flywheels used in space energy storage systems or terrestrial applications. The system includes two radial passive magnet bearings and an active radial damper. The rotordynamic requirements of the system and its design are discussed and preliminary test results presented. Test results show that permanent-magnet radial bearings are well suited for high-speed rotors, such as flywheels, provided a small active radial damper is used to supplement system damping for traversing critical speeds and suppressing subsynchronous whirls.

Introduction

With no metal contact and no need of lubricant, magnetic bearings are ideal for supporting energy storage flywheel rotors operating in a vacuum environment. There are two kinds of magnetic bearings: an actively controlled type that uses electromagnets and a passive type that uses permanent magnets (PMs). The active type has stator poles with coils energized by power electronics that, in turn, are feedback-controlled by signals from displacement sensors. The active bearing not only requires electronics, sensors, and a power source, but also generates eddy-current and hysteresis heat on the rotor, which can only be dissipated by radiation in a vacuum. Therefore, rotor temperature may rise significantly above ambient and cause mechanical problems. Although it is possible to design an active bearing without poles [1] to minimize heat loss, the complexity of this type of bearing design remains.

Considering these aspects of the active bearing, the passive bearing would be the preferred choice, since it does not require any electronics or external power and generates insignificant heat on the rotor. However, although passive PM bearings are common [2, 3], they are seldom used for high-speed applications, such as flywheels. For a passive bearing to provide practical stiffness, PMs on both stator and rotor are required, and retention of the rotor magnets at high rotating speed is not a trivial design or fabrication challenge. Another concern for the rotordynamics is the lack of damping in the passive bearing. In the typical speed range of an energy storage flywheel (30,000 to 60,000 rpm), the shaft usually traverses two or more critical speeds and many structural resonance frequencies. Without proper system damping, the rotor risks vibration from synchronous and harmonic excitation due to unbalance, as well as catastrophic subsynchronous whirls.

For flywheels used in space energy storage systems or terrestrial applications, we are developing a passive system using two PM radial bearings. To supplement the system damping, a small active radial damper is included in the suspension system. The design of this passive system and experimental results are presented herein.

PM Radial Bearings

The two passive PM radial bearings consist of PM rings stacked axially [4, 5]. The rings on the rotor are clamped together with identical poles facing each other as shown in Figure 1. The magnets have the same polarity as those in stator, so that the magnetic flux is concentrated locally to enhance the repulsive bearing action. Since there are magnets on the shaft, special design considerations are needed to retain them at high speeds. Specifically, a radial preloaded stainless steel sleeve is used to

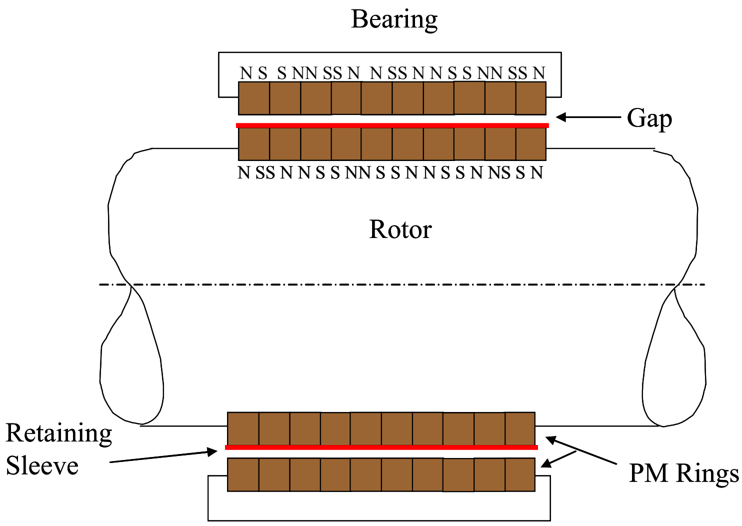

Figure 1. Axially Stacked PM Radial Bearing

support the rotor ring magnets. The preload keeps the magnets always in compression, even at high speeds.

Figure 2 shows several components of the PM radial bearing. The bearing includes 10 PM rings, with a rotor ring ID of 38.5 mm, a stator ring ID of 46.0 mm, a radial magnetic gap of 0.76 mm, and a PM ring cross section of 3 x 3 mm. The remnant flux density of the PM is 1.0 Tesla, and the bearing provides a measured radial stiffness of 263 N/mm (1500 lb/in.).

Since the PM thickness is relatively much smaller than the average radius, R, at the bearing gap, a 2-D finite-element static magnetic analysis was performed to predict bearing stiffness. Results of this analysis (Figure 3) indicated that repulsive force changes by 0.366 N for a gap change of 0.1 mm between the rotor and stator cross sections. This implies a linear stiffness $K_l = 0.366/0.1 = 3.66$ N/mm per mm of depth into the paper. It is readily proved that the bearing radial stiffness is:

$$K_r \approx \pi R\, K_l = \pi(22.62)(3.66) = 262 \text{ N/mm}$$

The analytical prediction is close to the measured stiffness. Assuming there is no ferromagnetic material close to the PM bearing, there is a negative axial stiffness (K_a) equal to $-2\,K_r$ or -524 N/mm associated with this positive radial stiffness. The active thrust bearing compensates for the negative stiffness.

The ID hoop stress of the rotor PM ring is about 172 x 10^6 Pa (25 ksi) at 66,000 rpm, much higher than the tensile strength of the neodymium-iron-boron magnet material (12 ksi) used in this application. Therefore, a radial preloaded Inconel sleeve of 0.5-mm thickness is used to support the rotor ring magnets. Since the radial gap is 0.75 mm, the rotor can only move radially 0.25 mm, and the corresponding load capacity is therefore 65 N (=263 x 0.25).

Spin tests for the PM bearings were conducted to 66,000 rpm in a commercial spin pit with no degradation of mechanical integrity or stiffness. Our experimental results confirmed that the amount of eddy-current damping generated with the copper sleeve (Figure 2) is low and likely inadequate for controlling transient vibrations, such as traversing a critical speed or dampening shock response. A separate radial passive damper of eddy-current type has been used before; it consists of a conducting disk with its outer edge rotating in a uniform axial magnetic field. Radial vibration of the disk would generate eddy current loss, which tends to dampen the vibration. However, unlike active magnetic bearings, where the damping can, within limits, be adjusted as needed, the damping in passive magnetic bearings or eddy dampers is limited in value and fixed by design.

Figure 2. PM Bearing Components

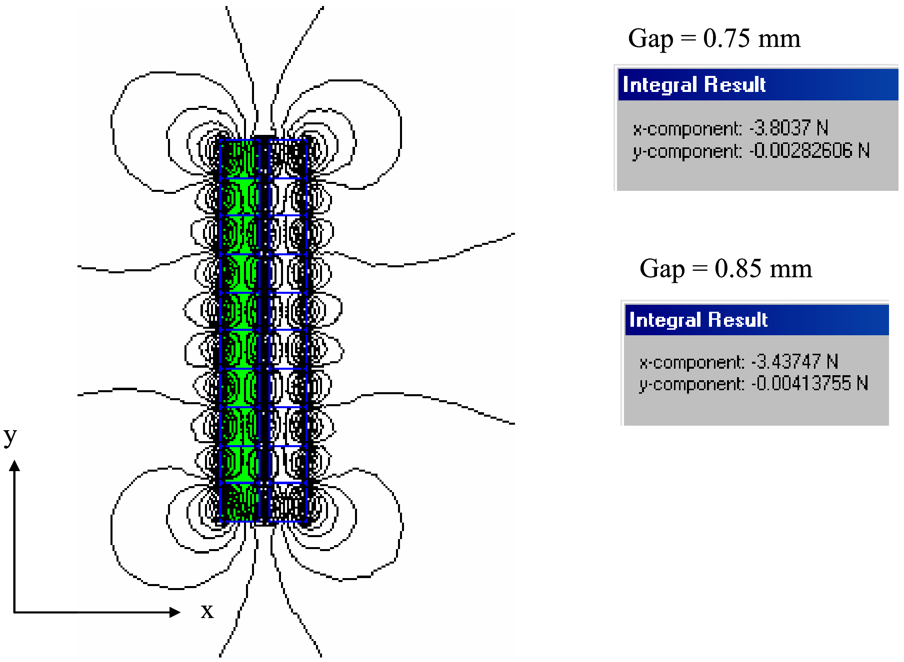

Figure 3. Results of 2-D Finite Element Analysis

Active Magnetic Radial Damper

An active radial damper is used in the system instead of an active radial bearing to replace one of the passive bearings, because the active damper does not take radial load and can be made small. We may choose dc current bias for the damper, and this would make the passive radial system fail-safe in the event of power loss.

To design an active damper for our test rotor with PM bearings, we performed a critical speed analysis of the dynamic system using DyRoBeS™ , a commercial rotordynamics program. The resulting critical speed map indicated that below 60,000 rpm there are only two rigid-body critical speeds at about 1900 rpm and 3800 rpm. As shown in Figure 4, the first bending critical is at 81,000 rpm. At the chosen location of the damper, there are plenty of vibration mode shape displacements, and therefore the damper will be effective in controlling the vibration.

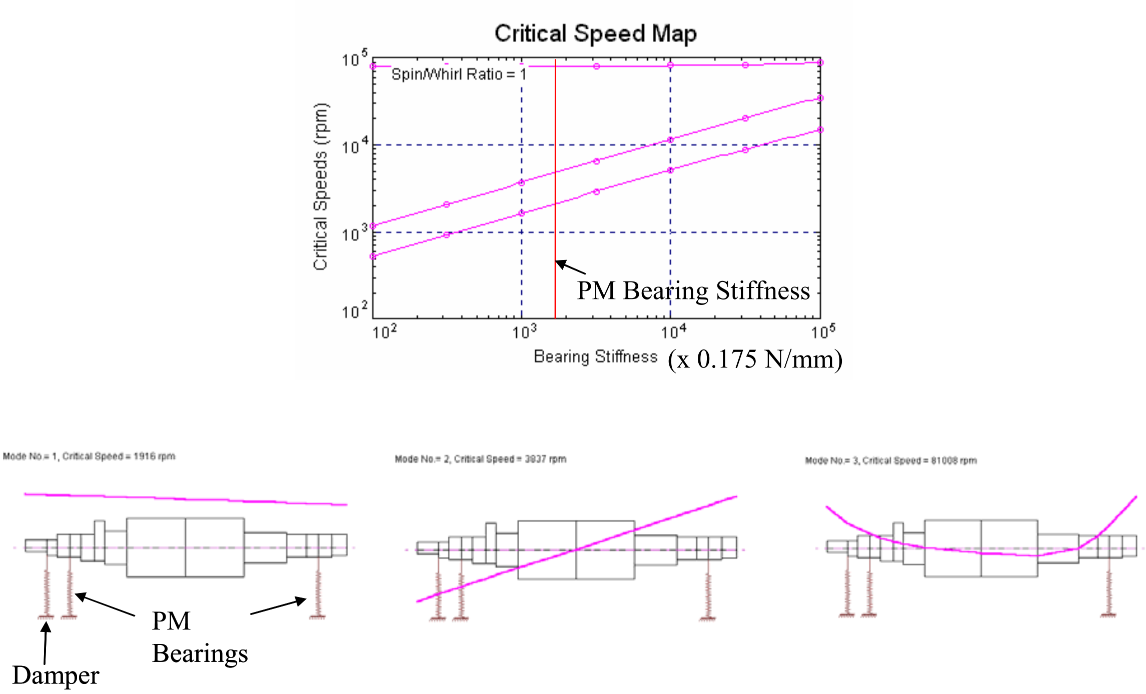

Figure 4. Test Rotor Critical Speeds

For testing convenience and safety reasons, the test rig rotor does not include a composite flywheel, and therefore misses a large polar moment of inertia. The gyroscopic stiffening effect of the inertia would have raised the second critical speed (with a conical mode shape) considerably. The first bending critical speed would also rise slightly due to the gyroscopic effect. The bending critical mode is too high in frequency and beyond the control bandwidth of the damper. We therefore implemented a notch filter in the damper controller to exclude the bending mode response from control feedback.

A damping coefficient of 0.875 N-sec/mm (5 lb-sec/in.) was chosen for the damper. It results in a log decrement value of 0.9 at the first critical speed, which is well above 0.4, an acceptable value in the machinery industry.

To size the damper, assume that the orbit at traversing the first critical is no more than 0.05 mm 0-pk (0.002 in. 0-pk). The maximum damper transient force is then about 8 N (≈ 0.875 N-sec/mm x 0.05 mm x 200 radian/sec). To minimize the number of poles and thus eddy-current loss, we selected a one-sided homopolar electromagnetic device with PM bias (see Figure 5). The laminated (silicon steel) pole area is 8 x 8 mm, and the laminated journal is 25 mm in diameter. The PM bias flux at the poles was measured to be 5.5 kGs. The damper has a force capacity of 24 N, which is three times larger than the predicted maximum load.

Active Magnetic Thrust Bearing

According to Earnshaw's theory [6], a rotor cannot be stabilized by passive bearings alone. At least one of the five degrees of freedom must be supported by an active or mechanical bearing. In this system, an actively controlled magnetic thrust bearing provides such support.

The thrust magnetic bearing works against the negative axial stiffness due to the PM radial bearings, about -10.5×10^5 N/m, in addition to the rotor weight of 16 kg. A conventional thrust bearing design is used, which includes a rotating disk and two single-coiled stators for push-and-pull actuation. The thrust bearing has a load capacity of 600 N, a thrust disk OD of 88 mm, a thrust disk ID of 45 mm, and an air gap of 0.5 mm. There are 150 coil turns per stator, with a resistance of 2 Ω per coil and a nominal gap inductance of 15 mH/coil.

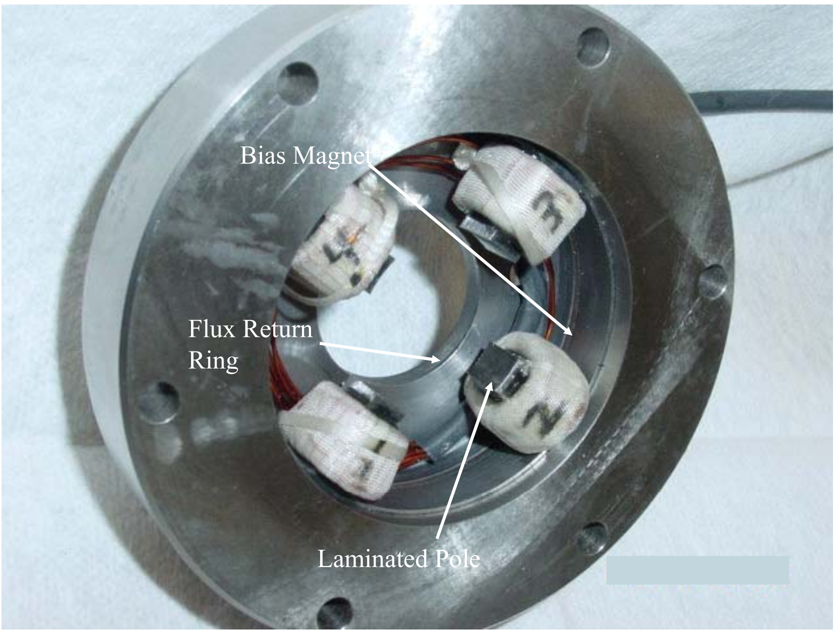

Figure 5. Four-pole Active Radial Damper

A conventional PID (proportional-integral-derivative) control algorithm is used to stabilize the thrust bearing. We plan to achieve a zero-power state for the thrust bearing, using a unique sliding-mode control (SMC) algorithm [7, 8] with automatic reference shift. At the zero-power state, there will be no dc current in the thrust coil, thus low copper loss.

The SMC performs feedback control of the rotor axial position based on a switching function:

$$S = C(Y - \delta) + Y' \qquad (1)$$

C is a positive weighing constant, and Y and Y' represent the rotor axial displacement and velocity, respectively. Changing the weighing constant, C, modifies the system damping, i.e., more damping with smaller C.

Using current-source power amplifiers, the coil current becomes essentially the control variable. The maximum current is that required to lift the rotor off a backup bearing.

The control current is calculated as:

$$I = -K\,|Y - \delta|\, S/|S| \qquad (2)$$

K is a positive current constant, and larger K means tighter control of error

$$\delta = C_i \int I\, dt \qquad (3)$$

C_i is a proportional constant. We call δ the control displacement reference shift, which is proportional to the integral of the control current. The control tries to shift its reference to a new position until the dc control current diminishes.

We will only energize one coil at a time, i.e., the top coil current = I as calculated by (2) and bottom coil current = 0, if I > 0. Otherwise, the top coil current = 0 and the bottom coil current = I.

Using C = 200 and K = 3000, a liftoff transient simulation of the test rotor under sliding mode thrust control was performed, with the results presented in Figure 6. The calculated displacement plot shows that the rotor rapidly settles to a position of 0.15 mm above the thrust bearing equilibrium point. Note that (0.15 mm)(1050 N/mm) = 158 N = 16 kg = rotor weight.

The current plot shows small regulating currents on the top or bottom coil. The effect of current constant K value on the transient currents will be evaluated in future axial dynamic testing.

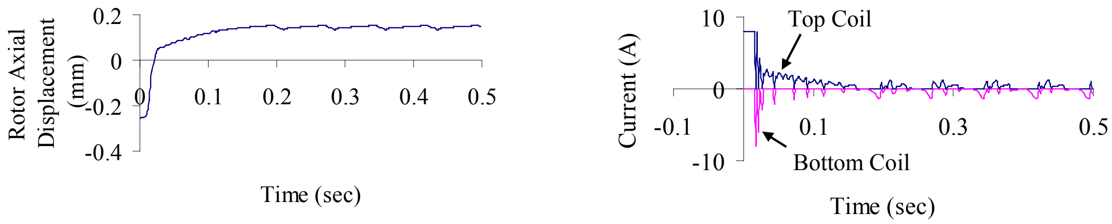

Figure 6. Thrust Bearing SMC Simulation

Rotordynamic Testing

Shown in Figure 7, the bearing-damper system test rig includes a 16-kg rotor, 525 mm long and oriented vertically. From the figure, one may appreciate the small size of the active damper as compared to the other components. Preliminary tests of the fully levitated rotor showed the first critical speed at 1900 rpm with a bouncing mode and the second critical speed at 3900 rpm with a conical mode. Both critical speeds are very close to analytically predicted values.

It took 50 min for the rotor to coast down from 5000 rpm in air. The damper and bearings have apparently very low power loss. It was very clear that without activating the damper the rotor would not be stable above the second critical speed.

The test rig was installed in a containment chamber for high-speed spin tests, and the rotor run up to 51,000 rpm. From the results of these tests, Figure 8 presents a typical frequency spectrum coastdown plot using a "peak-hold" mode in the frequency analyzer. The high-speed rotor displacement (mostly due to probe runout) is very flat, because the rotor runs at the mass center with soft PM bearings. Figures 9 and 10 shows frequency spectra of a rotor top probe at rotor speeds of 20, 30, 40, and 51 krpm. The subsynchronous shaft vibration at the first critical frequency apparently grew with the speed. The excitation appears aerodynamic in nature. In other words, the PM bearings may have functioned as unloaded plain cylindrical air bearings and generated destabilizing cross-coupling stiffness [9, 10], which is proportional to speed. One would expect the excitation does not exist in a vacuum chamber as for most flywheel applications.

Summary and Conclusions

Design and test results have been presented for a passive magnetic bearing system including two PM radial bearings, an active magnetic radial damper, and an active magnetic thrust bearing. The radial part of the bearing system is simple in control and efficient in power consumption. Test results show that PM radial bearings are well suited for high-speed rotors, such as flywheels, provided a small active radial damper is used to supplement system damping for traversing critical speeds and suppressing sub-synchronous whirls. Further, results of our analysis show that the thrust bearing can be controlled to achieve the zero-power state using a SMC algorithm, which further reduces system bearing energy consumption.

Acknowledgments

This work has been supported by NASA under a Phase II Small Business Innovation Research (SBIR) contract NAS3-02128.

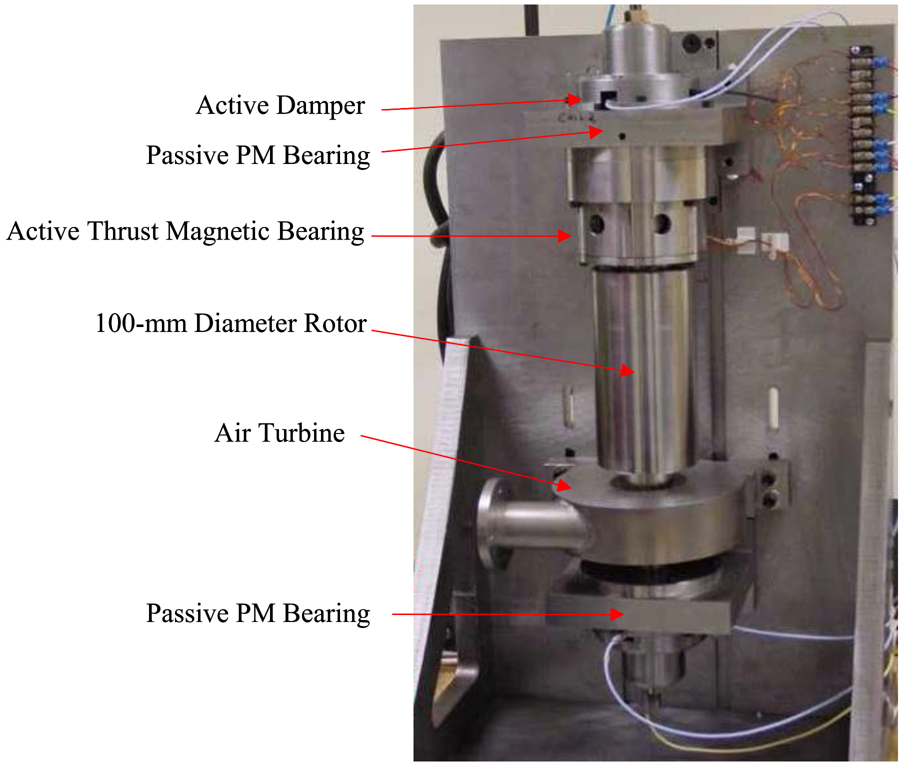

Figure 7. PM Bearing and Active Damper Test Rig

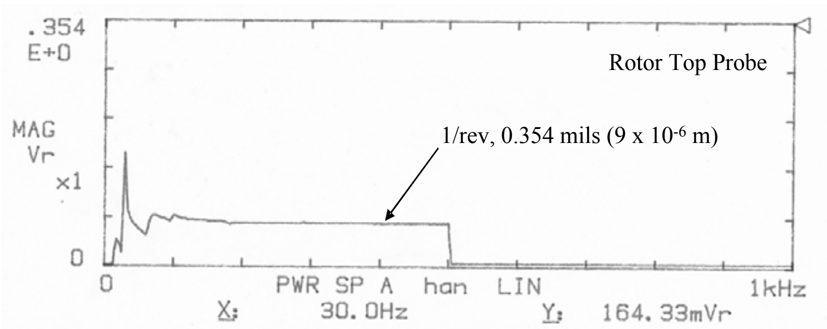

Figure 8. Typical Frequency Spectrum Coastdown Plot from 30,000 rpm

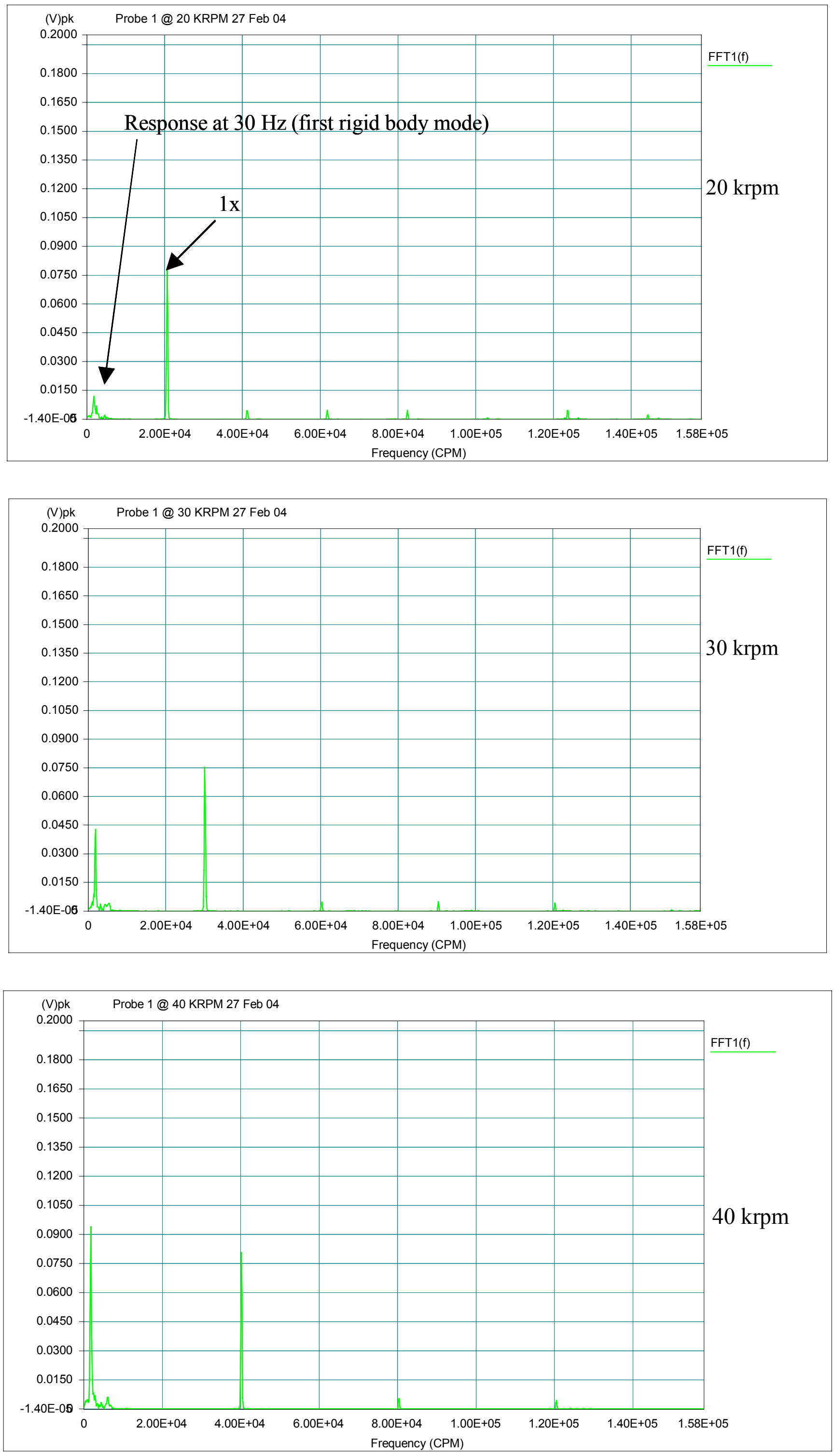

Figure 9. Displacement Frequency Spectra at 20, 30, and 40 krpm

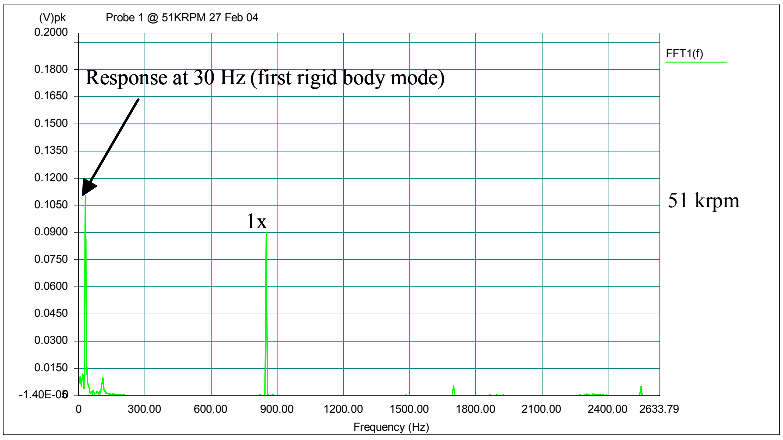

Figure 10. Displacement Frequency Spectra at 51 krpm

References

1. Chen, H. M. "A Stator-Controlled Magnetic Bearing." Presented at 6th Int'l Symp. on Mag. Brg., Cambridge, MA, August 5-7, 1998.
2. Chen H. M., W. Smith, and J. Walton. "A High Efficiency Magnetic Bearing for a Rotary Blood Pump." ASAIO 44th Annual Conference, New York, NY, October 1998.
3. Chen, H. M. et al. "Development of Magnetically Levitated Blood Pumps." 6th Int'l Symp. on Mag. Susp. Tech., Turin, Italy, October 7-11, 2001, pp. 30-36.
4. Yonnet, J. "Permanent Magnet Bearings and Couplings." IEEE Transactions on Magnetics, Vol. Mag-17, No.1, January 1981.
5. Yonnet, J., et al. "Stacked Structures of Passive Magnetic Bearings." J. Appl. Phys. 70(10), November 1991.
6. Earnshaw, S. "On The Nature Of The Molecular Forces Which Regulate The Constitution Of The Lumiferous Ether." Trans. Camb. Phil. Sec. 7 (1842), 97-112.
7. Utkin, V., J. Guldner, and J. Shi. Sliding Mode Control in Electromechanical Systems. Taylor & Francis, 1999.
8. Allaire, P.E. and A. Sinha. "Robust Sliding Mode Control of a Planar Rigid Rotor System on Magnetic Bearings." 6th Int'l Symp. on Mag. Brg, Cambridge, MA, August 5-7, 1998.
9. Lee, C. W. Vibration Analysis of Rotors. Chapter 3, Kluwer Academic Publishers, 1993.
10. Ehrich, F.F. Handbook of Rotordynamics. McGraw-Hill Inc., 1992.